



Article

Magnetofluorescent Nanocomposite Comprised of Carboxymethyl Dextran Coated Superparamagnetic Iron Oxide Nanoparticles and β -Diketon Coordinated Europium Complexes

Daewon Han ¹, Seung-Yun Han ², Nam Seob Lee ², Jongdae Shin ^{1,3}, Young Gil Jeong ², Hwan-Woo Park ^{1,3,*} and Do Kyung Kim ^{2,*}

¹ Department of Cell Biology, Konyang University College of Medicine, Daejeon 302-718, Korea; eodnjs0319@naver.com (D.H.); shinjd@konyang.ac.kr (J.S.)

² Department of Anatomy, College of Medicine, Konyang University, Daejeon 302-718, Korea; jjzzy@konyang.ac.kr (S.-Y.H.); nslee@konyang.ac.kr (N.S.L.); ygjeong@konyang.ac.kr (Y.G.J.)

³ Myunggok Medical Research Institute, Konyang University College of Medicine, Daejeon 302-718, Korea

* Correspondence: hwanwoopark@konyang.ac.kr (H.-W.P.); dokyung@konyang.ac.kr (D.K.K.); Tel.: +82-42-600-8677 (H.-W.P.); +82-42-600-6445 (D.K.K.)

Received: 10 December 2018; Accepted: 29 December 2018; Published: 4 January 2019



Abstract: Red emitting europium (III) complexes $\text{Eu}(\text{TFAAN})_3(\text{P}(\text{Oct})_3)_3$ (TFAAN = 2-(4,4,4-Trifluoroacetoacetyl)naphthalene, $\text{P}(\text{Oct})_3$ = trioctylphosphine) chelated on carboxymethyl dextran coated superparamagnetic iron oxide nanoparticles (CMD-SPIONs) was synthesized and the step wise synthetic process was reported. All the excitation spectra of distinctive photoluminesces were originated from f-f transition of Eu^{III} with a strong red emission. The emission peaks are due to the hypersensitive transition $^5\text{D}_0 \rightarrow ^7\text{F}_2$ at 621 nm and $^5\text{D}_0 \rightarrow ^7\text{F}_1$ at 597 nm, $^5\text{D}_0 \rightarrow ^7\text{F}_0$ at 584 nm. No significant change in PL properties due to addition of CMD-SPIONs was observed. The cytotoxic effects of different concentrations and incubation times of $\text{Eu}(\text{TFAAN})_3(\text{P}(\text{Oct})_3)_3$ chelated CMD-SPIONs were evaluated in HEK293T and HepG2 cells using the WST assay. The results imply that $\text{Eu}(\text{TFAAN})_3(\text{P}(\text{Oct})_3)_3$ chelated CMD-SPIONs are not affecting the cell viability without altering the apoptosis and necrosis in the range of 10 to 240 $\mu\text{g}/\text{mL}$ concentrations.

Keywords: europium complexes; superparamagnetic; iron oxide nanoparticles; magnetofluorescent

1. Introduction

Non-invasive fluorescent [1] probes are required to evaluate the efficacy of the drug at the molecular level. The evaluation of the efficacy of the drug is also important from a biological point of view, as it traces the specific expression after administrating the drug into the cells [2]. Among these probes, fluorescence probes are excellent for tracking light emitted from the molecules after excitation at a specific wavelength because they have high sensitivity and spatial resolution [3]. One of the most important factor in selecting a bioimaging probe is the organic molecules/particles needed to be easily localize/internalize to particular organelles or sub-cellular sites. Currently, optical probes are classified into two categories; one is organic molecules such as fluorescein isothiocyanate (FITC) [4], Alexa Fluor [5], tetramethylrhodamine (TRITC) [6], cyanine (Cy3, Cy5, and Cy7), green fluorescent protein (GFP), yellow fluorescent protein (YFP), and cyan fluorescent protein (CFP), etc., while the other consists of inorganic materials/quantum dots (QDs), such as CdSe/ZnS [7], InP/ZnS [8], CuInS/ZnS [9], and $\text{CH}_3\text{NH}_3\text{PbX}_3$ (X = Cl, Br, I) [10], etc.

QDs are very commonly used materials in biomedical applications such as in detection, biomarkers, and imaging agents. However, the ineffective uptake of QDs in living cells is an obstacle

to its use in nanomedicine. A high dose of QDs is required to resolve the low localization in living cells. It is therefore significant to realize and strategy of designing an effective QDs for biomedical uses by understanding the permeability of cell membranes depending on the substances and functional groups present on the QD surface [11].

The synthesis of lanthanide complexes, which is a substance that emits light under ultraviolet light, has been extensively studied because of its broad range of applications. In recent years, the lanthanide complexes have been intensively investigated in nanomedicine because of their strong characteristics against anti-photobleaching compared with conventional fluorescent materials. They can be used in diagnostic kit, micro chemical detections, cell labeling, and other applications, because of their low cytotoxicity and high quantum yield [12].

At present, magnetic nanoparticles have been developed to improve the diagnosis and therapeutic effects of various diseases, and they are the most studied materials among nano-sized materials developed to date. Superparamagnetic iron oxide nanoparticles (SPION) have inherent beneficial characteristics, including magnetic properties, magnetized under external magnetic field, biocompatibility, high dispersivity after coating with biocompatible substance, cellular uptake, and a short blood half-life. These benefits are the most effective parameters for transporting drugs, proteins, and probes for nanomedicinal applications [13,14].

In this work, we try to develop a multi-purpose nanoprobe called magnetofluorescent [15,16] nanoparticles that can be traced noninvasively by MRI in-vivo and by confocal microscope in-vitro. SPIONs were prepared in the presence of dextran molecules and carboxymethyl group was activated with monochloroacetic acid followed by crosslinking the dextran (CLD) molecules with epichlorohydrin to cage-like structure tightly grafted on SPIONs. Finally, β -diketon coordinated europium complexes composed of 2-(4,4,4-trifluoroacetoacetyl)naphthalene (TFAAN), trioctylphosphine (P(Oct)₃), and Eu^{III} were chelated on CLD-SPION.

2. Materials and Methods

2.1. Chemicals

Ferric chloride hexahydrate (FeCl₃·6H₂O), ferrous chloride tetrahydrate (FeCl₂·4H₂O), ammonium hydroxide solution (28% in water), europium chloride hexahydrate (EuCl₃·6H₂O), trioctylphosphine (P(Oct)₃), 3-[4,5-dimethylthiazol-2-yl]-2,5-diphenyltetrazolium bromide (MTT), and ethanol dialysis tubing cellulose membrane with a weight-cutoff (MWCO = 12,400) were purchased from Sigma-Aldrich Chemical Co. (St. Louis, MO, USA). Tokyo Chemical Industry Co. Ltd (Tokyo, Japan) supplied the 2-(4,4,4-Trifluoroacetoacetyl)naphthalene (TFAAN). Dextran T-10, epichlorohydrin and monochloroacetic acid (MCA) were supplied by DaeJung Chemicals and Metals Co. Ltd. (Kyunggi do, South Korea).

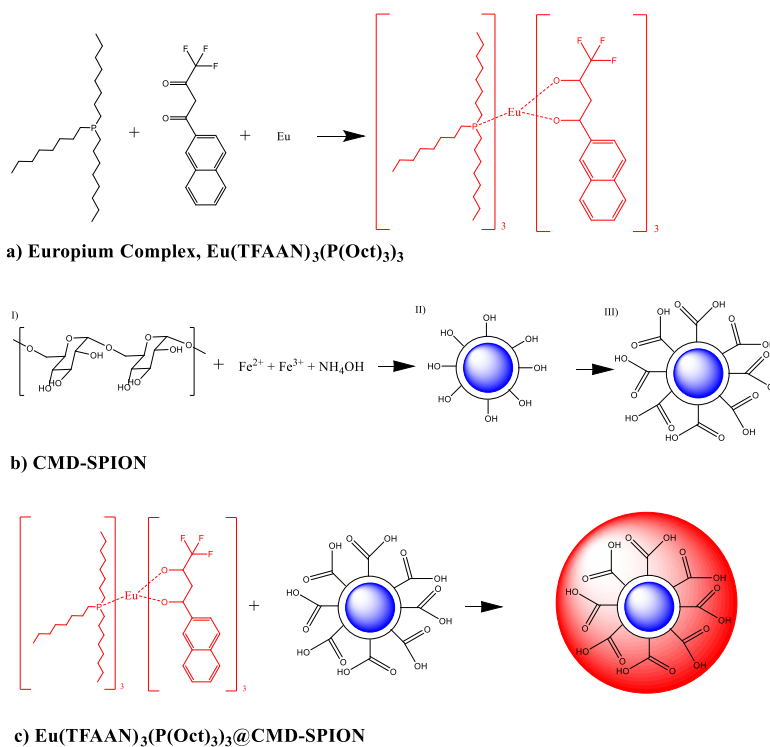
2.2. Characterization

The particle size, morphology, and distribution quality of Eu(TFAAN)₃(P(Oct)₃)₃ on CMD-SPION nanospheres were analyzed by Hitachi H-7650 TEM (EVISA, Tokyo, Japan). Fourier transform infrared (FT-IR) spectra were recorded using an ALPHA FT-IR Spectrometer equipped with Platinum ATR (Bruker, Billerica, MA, USA). Excitation and emission spectra were examined by fluorospectrophotometer (RF-5301PC Shimadzu, Kyoto, Japan) equipped with a 150 W xenon discharge lamp as a light source. Cells were observed using LSM 510 confocal laser scan microscope (Zessi, Inc., San Diego, CA, USA) and E800 epifluorescence microscopic (Nikon, Inc., Tokyo, Japan).

2.3. Synthesis of β -Diketon Coordinated Europium Complexes

Europium complexes [17,18], Eu(TFAAN)₃(P(Oct)₃)₃, was prepared based on previously reported method with a minor modification. Europium chloride hexahydrate (EuCl₃·6H₂O, 0.366 g, 1 mmol) was dissolved in 50 mL distilled H₂O. In similar way, 2-(4,4,4-Trifluoroacetoacetyl)naphthalene (TFAAN,

0.266 g, 1 mmol) and trioctylphosphine ($P(\text{Oct})_3$, 0.370 g, 1 mmol) were dissolved in 50 mL EtOH. The final concentration of each stock solutions were 0.02 mmol. From the stock solution, 2 mL Eu^{3+} , 6 mL TFAAN, 6 mL $P(\text{Oct})_3$, and 100 μL (28% in water) NH_4OH were transferred to 20 mL glass bottle with a capped tightly and the temperature was increased to 60 °C in a water bath under magnetic stirring. The product was precipitated by centrifuge, washed three times with distilled H_2O and dried in vacuum oven at 70 °C for 24 h. The chemical structure of $\text{Eu}(\text{TFAAN})_3(\text{P}(\text{Oct})_3)_3$ is shown in Scheme 1a.



Scheme 1. Schematic illustration of (a) formation of europium complexes with 2-(4,4,4-Trifluoroacetoacetyl)naphthalene (TFAAN) and trioctylphosphine ($P(\text{Oct})_3$), (b) in-situ synthesis of superparamagnetic iron oxide nanoparticles (SPIONs) in dextran matrix, crosslinking the dextran molecules with epichlorohydrin and activation of carboxymethyl group with monochloroacetic acid; (c) chelation of $\text{Eu}(\text{TFAAN})_3(\text{P}(\text{Oct})_3)_3$ on CMD-SPION.

2.4. In situ Synthesis of Dextran Coated Superparamagnetic Iron Oxide Nanoparticles by Co-Precipitation

Scheme 1b shows the overall procedure to prepare the CMD-SPIONs. N_2 gas was directly flowed into the solution for 30 min to remove the oxygen before the experiments. 5.46 g Iron(III) chloride hexahydrate and 1.99 g iron(II) chloride tetrahydrate were dissolved in 90 mL H_2O and 500 μL concentrated HCl by heating at 60 °C in a water bath until all the salt was fully dissolved. After a transparent solution was achieved, the solution was topped up with H_2O to make a final volume of 100 mL to prepare the iron stock solution ($[\text{Fe}^{2+}] = 200 \text{ mM}$, $[\text{Fe}^{3+}] = 100 \text{ mM}$). After this, 1 g Dextran T-10 (Mw 10,000) was dissolved in 10 mL iron stock and add 90 mL H_2O . After the dextran was fully dissolved, the solution was placed in an ice bath for 30 min. 10 mL concentrated ammonia was added dropwise under magnetic stirring and kept for 30 min. The temperature of the mixture was increased to 70 °C and kept for an additional 30 min. After the product was cooled to 25 °C (R. T.), the black solid was recovered by neodymium magnet and the supernatant was eliminated by decantation. The solid precipitate was washed 5 times with H_2O to remove unreacted salts and by-products. The final product, called SPIONs, was dispersed in 100 mL H_2O by probe sonicate for 1 min in an ice bath to form an extremely stable colloidal solution. Crosslinking between the dextran molecules surrounding on SPIONs was performed to attach the dextran more steadily by

following process; 10 mL 5 M NaOH was added in stock solution of SPIONs under vigorous magnetic stirring. 5 mL epichlorohydrin was added into the mixture and kept for 24 h at 25 °C under vigorous shaking by the shaker to avoid the phase separation between aqueous and organic layer. The constant shaking stimulates the chemical reaction between two different phases. After finalizing the reaction, the mixture solution was poured in dialysis tubing cellulose membrane with a weight-cutoff (MWCO = 12,400) and dialyzed against 5 L distilled H₂O. The distilled H₂O was changed with fresh one every 1 h for 5 times and left overnight. The conductivity of the H₂O was monitored by a conductivity meter to regulate the termination point of the washing progression. The solution was concentrated by vacuum dryer until a final volume of 20 mL and remarked as CLD-SPIONs. To activate the carboxylic group in dextran, carboxymethylation was accomplished through the following process; 10 mL 0.1 M NaOH was mixed with 10 mL CLD-SPIONs under magnetic stirring for 30 min at 25 °C while directly purging N₂. After this, 0.443 MCA was added dropwise to the solution, and the temperature was increased to 60 °C in an oil bath and kept for 60 min while N₂ was flowing. After the reaction was completed, CMD-SPIONs was dialyzed against 5 L distilled H₂O to remove the impurities and kept at 4 °C.

2.5. Magnetofluorescent Composite of Eu(TFAAN)₃(P(Oct)₃)₃@CMD-SPIONs

30 mg CMD-SPIONs in 10 mL deionized water was added in 1 mg Eu(TFAAN)₃(P(Oct)₃)₃ in 10 mL EtOH and heated to 80 °C in oil bath under magnetic stirring for 1 h. The sample was dialyzed against 5 L deionized water using a membrane tubing with a molecular cut-off 12,500 for three consecutive periods of 8 h. The final chemical structure of Eu(TFAAN)₃(P(Oct)₃)₃@CMD-SPIONs is shown in Scheme 1c.

2.6. Cell Culture

Human embryonic kidney (HEK) 293T cells and human liver cancer cell line HepG2 cells were cultured in Dulbecco's Modified Eagle's Medium (DMEM, Welgene, Gyeongsangbuk-do, Korea) supplemented with 10% fetal bovine serum (FBS, Welgene, Korea) and 100 U/mL penicillin-streptomycin (Welgene, Korea). Culture conditions were maintained in a humidified atmosphere containing 5% CO₂ at 37 °C.

2.7. Immunofluorescence

HEK293T cells or HepG2 cells were seeded onto each coverslip with 3×10^5 cells per coverslip in 24-well culture plates and then grown to 80% confluence. The cells were treated with indicated concentrations of Eu(TFAAN)₃(P(Oct)₃)₃@CMD-SPIONs dissolved in water for indicated time periods. Coverslips were washed once with phosphate-buffered saline (PBS) and fixed with 4% paraformaldehyde. After washing, coverslips were mounted in 4',6-diamidino-2-phenylindole (DAPI, Invitrogen, Carlsbad, CA, USA) on glass slides. Samples were analyzed under an epifluorescence-equipped microscope (DM2500, Leica, Wetzlar, Germany).

2.8. Cytotoxicity Assay

Cell viability was measured using WST-1 assay (Daeil Lab Service) according to the standard protocol of the manufacturer. Briefly, HEK293T cells and HepG2 cells were plated in 96-well plates at a concentration of 1×10^4 cells/well and treated with indicated concentrations of Eu(TFAAN)₃(P(Oct)₃)₃@CMD-SPIONs for indicated time periods. After incubated, 10 µL of WST-1 solution was added to each well and incubated for 30 min at 37 °C under 5% CO₂ incubator. After this, optical density of 96-well plates was measured in a microplate reader (Bio-Rad) at 450 nm and the absorbance values of the treated cells were expressed as a percentage of the absorbance values of the control.

3. Results

Figure 1 shows TEM images of carboxymethyl dextran coated superparamagnetic iron oxide nanoparticles (CMD-SPIONs) and $\text{Eu}(\text{TFAAN})_3(\text{P}(\text{Oct})_3)_3$ conjugated on CMD-SPIONs. The average particle diameter of SPIONs was around 12 nm with an irregular shape. After conjugation of $\text{Eu}(\text{TFAAN})_3(\text{P}(\text{Oct})_3)_3$, the particles had some agglomeration. The gray molecules are $\text{Eu}(\text{TFAAN})_3(\text{P}(\text{Oct})_3)_3$, as shown in Figure 1b and can be eliminated by washing with ethanol by centrifuge or applying an external magnetic forces such as neodymium magnet.

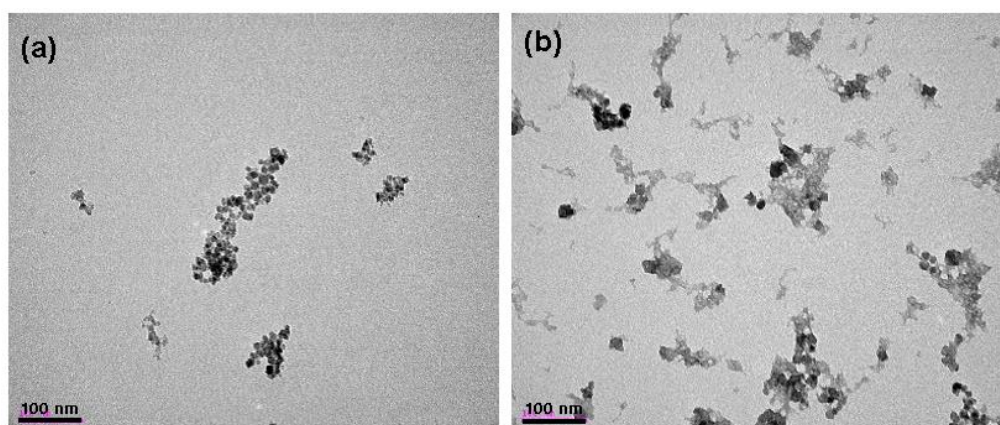


Figure 1. TEM images of (a) carboxymethyl dextran coated superparamagnetic iron oxide nanoparticles (CMD-SPIONs) and (b) $\text{Eu}(\text{TFAAN})_3(\text{P}(\text{Oct})_3)_3$ conjugated on CMD-SPIONs.

Differential scanning calorimetry (DSC) analysis was performed for CMD-SPION, $\text{Eu}(\text{TFAAN})_3(\text{P}(\text{Oct})_3)_3$, and $\text{Eu}(\text{TFAAN})_3(\text{P}(\text{Oct})_3)_3$ chelated CMD-SPIONs (Figure 2). DSC plot of CMD-SPION exhibited the endothermic peaks at 75 °C and 164.6 °C and exothermic peak at 136 °C, whereas $\text{Eu}(\text{TFAAN})_3(\text{P}(\text{Oct})_3)_3$ and $\text{Eu}(\text{TFAAN})_3(\text{P}(\text{Oct})_3)_3$ chelated CMD SPIONs did not appear at all. The temperature profile of $\text{Eu}(\text{TFAAN})_3(\text{P}(\text{Oct})_3)_3$ system showed the distinctive peak at 54 °C as it appeared in DSC curve of both $\text{Eu}(\text{TFAAN})_3(\text{P}(\text{Oct})_3)_3$ and $\text{Eu}(\text{TFAAN})_3(\text{P}(\text{Oct})_3)_3$ chelated CMD SPIONs.

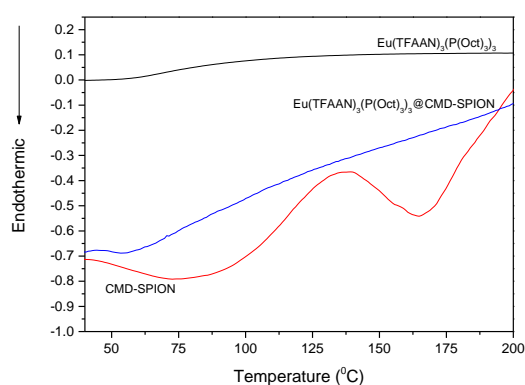


Figure 2. Differential scanning calorimetry analysis of CMD-SPION and $\text{Eu}(\text{TFAAN})_3(\text{P}(\text{Oct})_3)_3$ chelated CMD-SPIONs.

Figure 3 shows PL spectra of (a) emission and (b) excitation profiles depending on different concentration of $\text{Eu}(\text{TFAAN})_3(\text{P}(\text{Oct})_3)_3$ chelated on CMD-SPIONs. All the excitation spectra reveal a comparable tendency of distinctive photoluminesces (PL) coming from f-f transition of Eu^{III} with a strong red emission [19]. The maximum emission (EM) peak is due to the hypersensitive transition

$^5D_0 \rightarrow ^7F_2$ at 621 nm and $^5D_0 \rightarrow ^7F_1$ at 597 nm, $^5D_0 \rightarrow ^7F_0$ at 584 nm. No significant change in PL properties due to addition of CMD-SPIONs was observed.

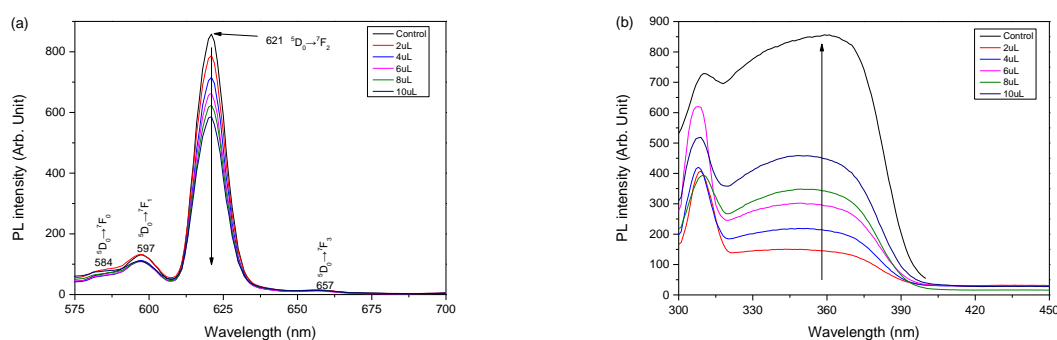


Figure 3. (a) Emission and (b) excitation spectra depending on different concentration of $\text{Eu}(\text{TFAAN})_3(\text{P}(\text{Oct})_3)_3$ chelated on CMD-SPIONs. Emission spectra were measured at the excitation wavelength of 360 nm and excitation wavelength of 621 nm.

Figure 4 shows zeta potentials of CMD-SPIONs and $\text{Eu}(\text{TFAAN})_3(\text{P}(\text{Oct})_3)_3$ chelated on CMD-SPIONs. Zeta (ζ) potential is used as a proper index for colloidal stability by evaluating the quantification of the magnitude of the surface charge on the particles [20], and the value is generally used to interpret and manipulate the stability of colloidal dispersion. The ζ -potentials of CMD-SPIONs is -17 mV and $\text{Eu}(\text{TFAAN})_3(\text{P}(\text{Oct})_3)_3$ chelated on CMD-SPIONs is changed to 9.7 mV.

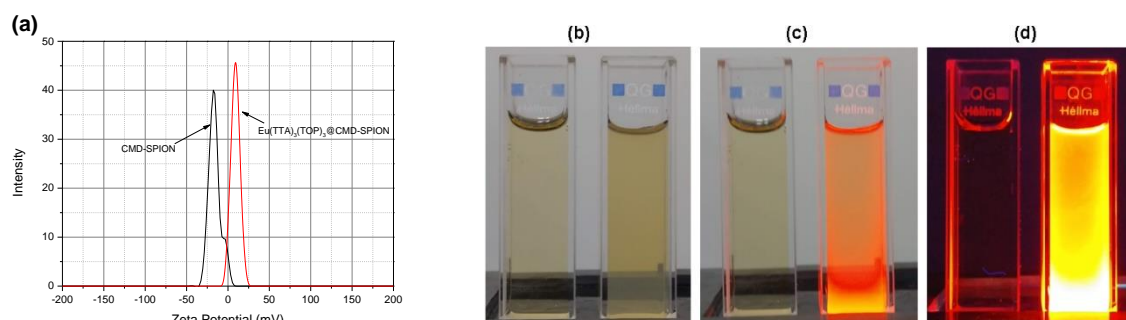


Figure 4. (a) Zeta Potentials of CMD-SPION and $\text{Eu}(\text{TFAAN})_3(\text{P}(\text{Oct})_3)_3$ chelated on CMD-SPIONs. Photograph images of CMD-SPION (left) and $\text{Eu}(\text{TFAAN})_3(\text{P}(\text{Oct})_3)_3$ chelated on CMD-SPIONs (right) dispersed in water under (b) daylight, (c) daylight + UV light at 365 nm, and (d) UV light at 365 nm.

Figure 5 shows FTIR spectra of $\text{Eu}(\text{TFAAN})_3(\text{P}(\text{Oct})_3)_3$, CMD-SPIONs and $\text{Eu}(\text{TFAAN})_3(\text{P}(\text{Oct})_3)_3$ chelated on CMD-SPIONs show absorption peaks around 3300 cm^{-1} coming from OH-stretching vibrations of water molecules and 2922 cm^{-1} can be allocated to the sp^3 bonding of C-H. In the CMD spectrum, deformation vibration $\delta(\text{C-OH})$ which appears at 1250 cm^{-1} and $\nu(\text{C-O})$ vibration around 1150 cm^{-1} . The absorption at 1462 cm^{-1} is attributed to C=C bond and 1688 cm^{-1} is assigned to C=O bond. The stretching vibration bands of P=O (1061 cm^{-1}) bond are appeared in $\text{Eu}(\text{TFAAN})_3(\text{P}(\text{Oct})_3)_3$ and $\text{Eu}(\text{TFAAN})_3(\text{P}(\text{Oct})_3)_3$ chelated on CMD-SPIONs. These results imply that $\text{Eu}(\text{TFAAN})_3(\text{P}(\text{Oct})_3)_3$ was successively grafted on magnetic nanoparticles.

The cytotoxic effects of concentrations and incubation times of $\text{Eu}(\text{TFAAN})_3(\text{P}(\text{Oct})_3)_3$ chelated CMD-SPIONs were evaluated in HEK293T and HepG2 cells using the WST assay. (Figure 6) Figure 6a shows the cytotoxic effects of HEK293T and HepG2 cells treated with the indicated concentration of $\text{Eu}(\text{TFAAN})_3(\text{P}(\text{Oct})_3)_3$ @CMD-SPIONs for 6 h. Cell viability was measured by WST-1 assay. Data are shown as mean \pm s.e.m. ($n = 3$). Figure 6b shows cytotoxic effects of HEK293T and HepG2 cells treated with $72\text{ }\mu\text{g/mL}$ $\text{Eu}(\text{TFAAN})_3(\text{P}(\text{Oct})_3)_3$ @CMD-SPIONs for indicated periods of time. Cell viability was measured by WST-1 assay. Data are shown as mean \pm s.e.m. ($n = 3$)

Figure 6c,d shows the results of HEK293T (c) and HepG2 cells (d) treated the indicated concentration of $\text{Eu}(\text{TFAAN})_3(\text{P}(\text{Oct})_3)_3$ @CMD-SPIONs for 24 h. The cells were stained with Muse Annexin V and Dead Cell reagent and then analyzed for apoptosis by the Muse Cell Analyzer.

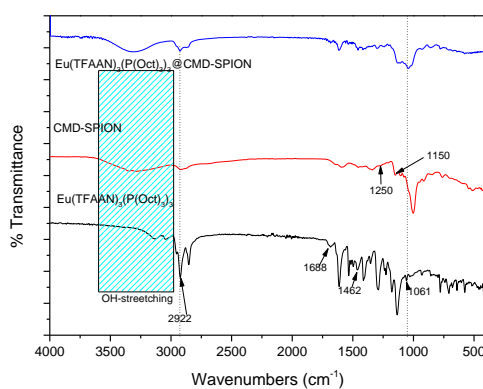


Figure 5. FT-IR spectra of $\text{Eu}(\text{TFAAN})_3(\text{P}(\text{Oct})_3)_3$, CMD-SPION and $\text{Eu}(\text{TFAAN})_3(\text{P}(\text{Oct})_3)_3$ chelated on CMD-SPIONs.

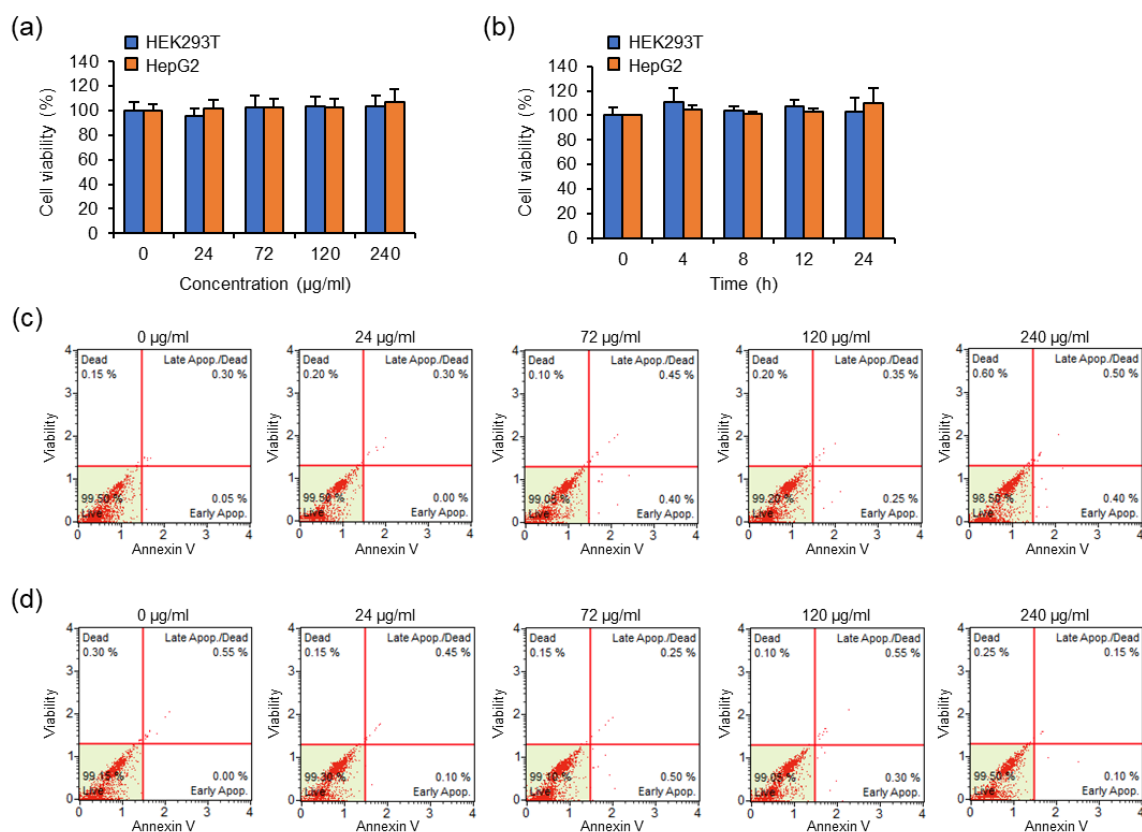


Figure 6. Cellular cytotoxicity of $\text{Eu}(\text{TFAAN})_3(\text{P}(\text{Oct})_3)_3$ @CMD-SPIONs in HEK293T and HepG2 cells. (a) HEK293T and HepG2 cells were treated with the indicated concentration of $\text{Eu}(\text{TFAAN})_3(\text{P}(\text{Oct})_3)_3$ @CMD-SPIONs for 6 h. Data are shown as mean \pm s.e.m. ($n = 3$) (b) HEK293T and HepG2 cells were treated with 72 $\mu\text{g}/\text{mL}$ $\text{Eu}(\text{TFAAN})_3(\text{P}(\text{Oct})_3)_3$ @CMD-SPIONs for indicated periods of time. Data are shown as mean \pm s.e.m. ($n = 3$) (c,d) HEK293T (c) and HepG2 cells (d) were treated the indicated concentration of $\text{Eu}(\text{TFAAN})_3(\text{P}(\text{Oct})_3)_3$ @CMD-SPIONs for 24 h.

Figure 7a,b shows intracellular uptake and distribution of $\text{Eu}(\text{TFAAN})_3(\text{P}(\text{Oct})_3)_3$ @CMD-SPIONs in HEK293T and HepG2 cells. Representative images of HEK293T (a) and HepG2 cells (b) treated with

vehicle (Control) or $\text{Eu}(\text{TFAAN})_3(\text{P}(\text{Oct})_3)_3\text{@CMD-SPIONs}$ at $72 \mu\text{g}/\text{mL}$ concentration for 4 h. Nuclei were stained with DAPI (blue). Scale bar, $20 \mu\text{m}$.

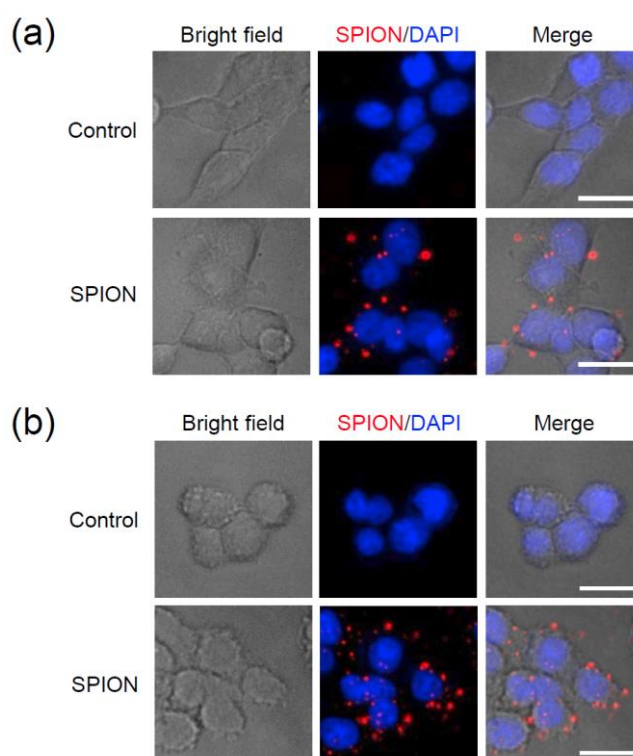


Figure 7. Intracellular uptake images of HEK293T (a) and HepG2 cells (b) treated with vehicle (Control) or $\text{Eu}(\text{TFAAN})_3(\text{P}(\text{Oct})_3)_3\text{@CMD-SPIONs}$. Nuclei were stained with DAPI (blue). Scale bar, $20 \mu\text{m}$.

4. Discussion

The crosslinking reaction of dextran [21] by epichlorohydrin happen in inter- or intra-molecular forms and are grafted on SPIONs surfaces. The dextran molecules are transformed from the surface of SPIONs into a strong and rigid structure, resulting in a heterogeneous solid structure on the SPIONs surface. The core-shell structure maintains the intermolecular bonding of physically bonded intermolecular materials and prevents separation in the aqueous solution. The epoxy moiety of epichlorohydrin alkylates OH groups and its epoxy group interacts with other OH groups of the dextran to form the corresponding inter- and intramolecular crosslinks.

In general, the magnetic nanoparticles have remanence magnetization even though it is classified as superparamagnetic material. The residual magnetic forces will induce the interactions between the magnetic particles resulting in large coagulation in the diameter range of 50–300 nm. To avoid the agglomeration, nonmagnetic substances were grafted on the surface of SPIONs. In this study, in situ formation of SPIONs was introduced to resolve the difficulties caused by coagulation during the synthesis of magnetic nanoparticles. Dextran molecules in the water form polymeric matrix and Fe^{2+} and Fe^{3+} ions are located in dextran molecules. In this manner, SPIONs nucleate inside the matrix and retain the distance among the particles while the particles are grown by thermal energy. The inter-particle forces due to the dipole-dipole interaction are adequate to elude the stimulus of residual magnetization resulting in forming exceptionally constant colloidal suspension. More benefits of using carbohydrate (i.e., dextran) are that it is biocompatible along with versatile derivatives by activation of specific functional groups. The DSC peak at $54 \text{ }^\circ\text{C}$ was disappeared because TFAAN and $\text{P}(\text{Oct})_3$ molecules were diffused into each other resulting in disappearing the endothermic and exothermic peaks, indicating that each molecule was changed into amorphous phase. In addition,

the mass of $\text{Eu}(\text{TFAAN})_3(\text{P}(\text{Oct})_3)_3$ is relatively larger than that of CMD-SPIONs when they are grafted and is not observed even with exothermic or endothermic peaks.

Approximately 20% of EM quenching was observed by comparing the EM intensity of $\text{Eu}(\text{TFAAN})_3(\text{P}(\text{Oct})_3)_3$ chelated on CMD-SPIONs and $\text{Eu}(\text{TFAAN})_3(\text{P}(\text{Oct})_3)_3$ at 621 nm. As the concentration of $\text{Eu}(\text{TFAAN})_3(\text{P}(\text{Oct})_3)_3$ against CMD-SPIONs was increased, ${}^5\text{D}_0 \rightarrow {}^7\text{F}_2$ was proportionally amplified with a virtually Gaussian shape.

The PL of $\text{Eu}(\text{TFAAN})_3(\text{P}(\text{Oct})_3)_3$ and $\text{Eu}(\text{TFAAN})_3(\text{P}(\text{Oct})_3)_3$ @CMD-SPIONs is analyzed by PL intensity ratio of ${}^5\text{D}_0 \rightarrow {}^7\text{F}_2$ and ${}^5\text{D}_0 \rightarrow {}^7\text{F}_1$. ${}^5\text{D}_0 \rightarrow {}^7\text{F}_1$ is comparatively strong [22], which corresponds to the magnetic dipole transition, has an independent intensity value inherently not affected by coordination environment. Therefore, the intensity values of the ${}^5\text{D}_0 \rightarrow {}^7\text{F}_1$ transition that are forbidden both for magnetic and electric dipole and can be used for comparison. In opposition, the intensity value of ${}^5\text{D}_0 \rightarrow {}^7\text{F}_2$ is an electric dipole transition affected by the physicochemical change values around the Eu^{III} .

ζ -potentials of CMD-SPIONs have a rather lower value but are extremely stable in water because CMD on SPIONs forms hyper branched matrix in water resulting in localization of SPIONs inside the net-like matrix. For this reason, CMD-SPIONs are exceptionally consistent without coagulation/flocculation even though the value of ζ -potentials is relatively low. The net electro charge on CMD-SPION shows opposite values after modifying the surface with $\text{Eu}(\text{TFAAN})_3(\text{P}(\text{Oct})_3)_3$. Figure 4b–d shows digital images of CMD-SPION (left) and $\text{Eu}(\text{TFAAN})_3(\text{P}(\text{Oct})_3)_3$ chelated on CMD-SPIONs (right) dispersed in water under (b) daylight, (c) daylight + UV light at 365 nm, and (d) UV light at 365 nm. $\text{Eu}(\text{TFAAN})_3(\text{P}(\text{Oct})_3)_3$ chelated on CMD-SPIONs exhibited quite bright luminescence with a red color under excitation with a UV light at 365 nm [23].

The cytotoxicity of 6 h after treatment with a different concentration of $\text{Eu}(\text{TFAAN})_3(\text{P}(\text{Oct})_3)_3$ chelated CMD-SPIONs (10 to 240 $\mu\text{g}/\text{mL}$) show that the cell viability in the range of 10 to 240 $\mu\text{g}/\text{mL}$ concentrations was more than 95%. $\text{Eu}(\text{TFAAN})_3(\text{P}(\text{Oct})_3)_3$ chelated CMD-SPIONs were not toxic to HEK293T and HepG2 cells even at a concentration of 240 $\mu\text{g}/\text{mL}$. At all time periods, no significant difference in cell viability was observed for all two cell types above when treated with $\text{Eu}(\text{TFAAN})_3(\text{P}(\text{Oct})_3)_3$ chelated CMD-SPIONs (Figure 6b). In addition, we determined the apoptotic effect of $\text{Eu}(\text{TFAAN})_3(\text{P}(\text{Oct})_3)_3$ chelated CMD-SPIONs in HEK293T and HepG2 cells by using Annexin V and dead cell reagent labeling flow cytometry. The four-quadrant plots in each panel show the necrotic cells (upper left), the late apoptotic cells (upper right), the viable cells (lower left), and the early apoptotic cells (lower right). Both cells treated with $\text{Eu}(\text{TFAAN})_3(\text{P}(\text{Oct})_3)_3$ chelated CMD-SPIONs revealed four-quadrant plots similar to those of the vehicle-treated cells (Figure 6c,d). These results indicate that $\text{Eu}(\text{TFAAN})_3(\text{P}(\text{Oct})_3)_3$ chelated CMD-SPIONs do not affect cell viability and do not alter the cell death program [24].

The intracellular uptake of $\text{Eu}(\text{TFAAN})_3(\text{P}(\text{Oct})_3)_3$ chelated CMD-SPIONs was evaluated in HEK293T and HepG2 cells using an epifluorescence-equipped microscopy. Internalization of $\text{Eu}(\text{TFAAN})_3(\text{P}(\text{Oct})_3)_3$ chelated CMD-SPIONs by HEK293T and HepG2 cells was not observed after 1 h incubation. After 6 h incubation, the cellular uptake of $\text{Eu}(\text{TFAAN})_3(\text{P}(\text{Oct})_3)_3$ chelated CMD-SPIONs in both cells occurred and was distributed within the cytoplasm (Figure 7). Since the europium complexes synthesized in this study have emission spectra at 619 nm when excited in the UV range, $\text{Eu}(\text{TFAAN})_3(\text{P}(\text{Oct})_3)_3$ chelated CMD-SPIONs do not require an additional red tracker.

5. Conclusions

We designed and synthesized a novel magnetofluorescent nanoprobe comprising of red emitting europium (III) complexes $\text{Eu}(\text{TFAAN})_3(\text{P}(\text{Oct})_3)_3$ chelated on carboxymethyl dextran coated CMD-SPIONs that can be traced noninvasively by MRI in-vivo and by confocal microscope in-vitro. All the excitation spectra distinctive photoluminesces came from f-f transition of Eu^{III} with a strong red emission. No significant change in PL properties due to addition of CMD-SPIONs was observed. The cell viability measured in HEK293T and HepG2 cells shows that $\text{Eu}(\text{TFAAN})_3(\text{P}(\text{Oct})_3)_3$ chelated

CMD-SPIONs do not affect cell viability and do not alter apoptosis and necrosis in the range of 10 to 240 µg/mL concentrations. At 4 h after incubation, the red fluorescence from Eu(TFAAN)₃(P(Oct)₃)₃ chelated CMD-SPIONs was mainly located in the cytoplasm with no significant cytotoxicity.

Author Contributions: H.-W.P. and D.K.K. designed the experiments and wrote the paper; D.H. performed the experiments and wrote the paper; S.-Y.H., N.S.L. and J.S. analyzed the data; Y.G.J. discussed the results.

Funding: This research was supported by grants from the National Research Foundation of Korea (NRF) funded by the Ministry of Science and ICT (No. NRF-2017R1A2B4005167) and the Ministry of Education (No. NRF-2017R1A6A1A03015713). This research was also supported by a grant of the Korean Health Technology R&D Project funded by the Ministry of Health & Welfare, Republic of Korea (No. HI17C1238).

Conflicts of Interest: The authors declare no conflict of interest.

References

1. Jiang, W.; Hong, C.; Wei, H.; Wu, Z.; Bian, Z.; Huang, C. A green-emitting iridium complex used for sensitizing europium ion with high quantum yield. *Inorg. Chim. Acta* **2017**, *459*, 124–130. [[CrossRef](#)]
2. Wang, L.; Li, B.; Xu, F.; Li, Y.; Xu, Z.; Wei, D.; Feng, Y.; Wang, Y.; Jia, D.; Zhou, Y. Visual in vivo degradation of injectable hydrogel by real-time and non-invasive tracking using carbon nanodots as fluorescent indicator. *Biomaterials* **2017**, *145*, 192–206. [[CrossRef](#)] [[PubMed](#)]
3. Gao, Y.; Pan, Y.; Chi, Y.; He, Y.; Chen, H.; Nemykin, V.N. A “reactive” turn-on fluorescence probe for hypochlorous acid and its bioimaging application. *Spectrochim. Acta Part A* **2019**, *206*, 190–196. [[CrossRef](#)] [[PubMed](#)]
4. Song, C.; Liu, J.; Li, J.; Liu, Q. Dual FITC lateral flow immunoassay for sensitive detection of Escherichia coli O157:H7 in food samples. *Biosens. Bioelectron.* **2016**, *85*, 734–739. [[CrossRef](#)] [[PubMed](#)]
5. Fecek, R.J.; Busch, R.; Lin, H.; Pal, K.; Cunningham, C.A.; Cuff, C.F. Production of alexa fluor 488-labeled reovirus and characterization of target cell binding, competence, and immunogenicity of labeled virions. *J. Immunol. Methods* **2006**, *314*, 30–37. [[CrossRef](#)] [[PubMed](#)]
6. Tran, N.B.N.N.; Knorr, F.; Mak, W.C.; Cheung, K.Y.; Richter, H.; Meinke, M.; Lademann, J.; Patzelt, A. Gradient-dependent release of the model drug TRITC-dextran from FITC-labeled BSA hydrogel nanocarriers in the hair follicles of porcine ear skin. *Eur. J. Pharm. Biopharm.* **2017**, *116*, 12–16. [[CrossRef](#)]
7. Zhao, M.; Chen, Y.; Han, R.; Luo, D.; Du, L.; Zheng, Q.; Wang, L.; Hong, Y.; Liu, Y.; Sha, Y. A facile synthesis of biocompatible, glycol chitosan shelled CdSeS/ZnS QDs for live cell imaging. *Colloids Surf. B. Biointerfaces* **2018**, *172*, 752–759. [[CrossRef](#)]
8. Chen, Y.; Yang, Y.; Ou, F.; Liu, L.; Liu, X.-H.; Wang, Z.-J.; Jin, L. InP/ZnS QDs exposure induces developmental toxicity in rare minnow (*Gobiocypris rarus*) embryos. *Environ. Toxicol. Pharmacol.* **2018**, *60*, 28–36. [[CrossRef](#)]
9. Zhang, F.; He, X.; Ma, P.; Sun, Y.; Wang, X.; Song, D. Rapid aqueous synthesis of CuInS/ZnS quantum dots as sensor probe for alkaline phosphatase detection and targeted imaging in cancer cells. *Talanta* **2018**, *189*, 411–417. [[CrossRef](#)]
10. Tsai, C.-H.; Lin, C.-M.; Kuei, C.-H. Improving the performance of perovskite solar cells by adding 1,8-diiodooctane in the CH₃NH₃PbI₃ perovskite layer. *Solar Energy* **2018**, *176*, 178–185. [[CrossRef](#)]
11. Argudo, P.G.; Martín-Romero, M.T.; Camacho, L.; Carril, M.; Carrillo-Carrión, C.; Giner-Casares, J.J. Fluorinated CdSe/ZnS quantum dots: Interactions with cell membrane. *Colloids Surf. B. Biointerfaces* **2019**, *173*, 148–154. [[CrossRef](#)] [[PubMed](#)]
12. Kaczmarek, M.T.; Zabiszak, M.; Nowak, M.; Jastrzab, R. Lanthanides: Schiff base complexes, applications in cancer diagnosis, therapy, and antibacterial activity. *Coord. Chem. Rev.* **2018**, *370*, 42–54. [[CrossRef](#)]
13. Nebu, J.; Anjali Devi, J.S.; Aparna, R.S.; Aswathy, B.; Lekha, G.M.; Sony, G. Fluorescence turn-on detection of fenitrothion using gold nanoparticle quenched fluorescein and its separation using superparamagnetic iron oxide nanoparticle. *Sens. Actuators B Chem.* **2018**, *277*, 271–280. [[CrossRef](#)]
14. Patil, R.M.; Thorat, N.D.; Shete, P.B.; Bedge, P.A.; Gavde, S.; Joshi, M.G.; Tofail, S.A.M.; Bohara, R.A. Comprehensive cytotoxicity studies of superparamagnetic iron oxide nanoparticles. *Biochem. Biophys. Rep.* **2018**, *13*, 63–72. [[CrossRef](#)] [[PubMed](#)]
15. Wen, Y.; Xu, M.; Liu, X.; Jin, X.; Kang, J.; Xu, D.; Sang, H.; Gao, P.; Chen, X.; Zhao, L. Magnetofluorescent nanohybrid comprising polyglycerol grafted carbon dots and iron oxides: Colloidal synthesis and

- applications in cellular imaging and magnetically enhanced drug delivery. *Colloids Surf. B. Biointerfaces* **2019**, *173*, 842–850. [[CrossRef](#)] [[PubMed](#)]
16. Tran, L.D.; Hoang, N.M.T.; Mai, T.T.; Tran, H.V.; Nguyen, N.T.; Tran, T.D.; Do, M.H.; Nguyen, Q.T.; Pham, D.G.; Ha, T.P.; et al. Nanosized magnetofluorescent Fe₃O₄–curcumin conjugate for multimodal monitoring and drug targeting. *Colloids Surf. Physicochem. Eng. Aspects* **2010**, *371*, 104–112. [[CrossRef](#)]
 17. Shin, J.D.; Lim, W.J.; Yu, K.S.; Lee, J.H.; Lee, N.S.; Jeong, Y.G.; Han, S.-Y.; Kim, D.K. Luminescent polystyrene latex nanoparticles doped with β-diketone europium chelate and methacrylic acid. *Eur. Polym. J.* **2016**, *83*, 89–98. [[CrossRef](#)]
 18. Dandekar, M.P.; Kondawar, S.B.; Itankar, S.G.; Nandanwar, D.V. Luminescence properties of electrospun nanofibers of europium complex Eu(TTA)₃phen/polymers. *Procedia Mater. Sci.* **2015**, *10*, 580–587. [[CrossRef](#)]
 19. Dandekar, M.P.; Itankar, S.G.; Kondawar, S.B.; Nandanwar, D.V.; Koinkar, P. Photoluminescent electrospun europium complex Eu(TTA)₃phen embedded polymer blends nanofibers. *Opt. Mater.* **2018**, *85*, 483–490. [[CrossRef](#)]
 20. Remya, N.S.; Syama, S.; Sabareeswaran, A.; Mohanan, P.V. Toxicity, toxicokinetics and biodistribution of dextran stabilized iron oxide nanoparticles for biomedical applications. *Int. J. Pharm.* **2016**, *511*, 586–598. [[CrossRef](#)]
 21. Easo, S.L.; Mohanan, P.V. Dextran stabilized iron oxide nanoparticles: Synthesis, characterization and in vitro studies. *Carbohydr. Polym.* **2013**, *92*, 726–732. [[CrossRef](#)] [[PubMed](#)]
 22. Ugale, A.; Kalyani, N.T.; Dhoble, S.J. Colour tunable emission from Eu_{0.5}Sm_{0.5}(TTA)₃ dpphen β-diketonate hybrid organic complex in various organic solvents. *Optik* **2018**, *171*, 171–182. [[CrossRef](#)]
 23. Yang, D.; Xu, Y.; Yao, Y.; Zhang, J.; Wang, J.; Wang, Y. A red light-emitting ionic europium (III) complex applied in near UV LED. *Synth. Met.* **2016**, *221*, 236–241. [[CrossRef](#)]
 24. Zou, Y.; Sun, F.; Liu, C.; Yu, C.; Zhang, M.; He, Q.; Xiong, Y.; Xu, Z.; Yang, S.; Liao, G. A novel nanotheranostic agent for dual-mode imaging-guided cancer therapy based on europium complexes-grafted-oxidative dopamine. *Chem. Eng. J.* **2019**, *357*, 237–247. [[CrossRef](#)]



© 2019 by the authors. Licensee MDPI, Basel, Switzerland. This article is an open access article distributed under the terms and conditions of the Creative Commons Attribution (CC BY) license (<http://creativecommons.org/licenses/by/4.0/>).